THESIS FOR THE DEGREE OF DOCTOR OF PHILOSOPHY
IN
THERMO AND FLUID DYNAMICS

Fuel Mixing in Gas-Solid Fluidized Beds: A Computational and Experimental Study

MEISAM FARZANEH KALOORAZI

Division of Fluid Dynamics

Department of Applied Mechanics

CHALMERS UNIVERSITY OF TECHNOLOGY

Göteborg, Sweden, 2013

Fuel Mixing in Gas-Solid Fluidized Beds:
A Computational and Experimental Study
MEISAM FARZANEH KALOORAZI
ISBN 978-91-7385-905-9

Doktorsavhandling vid Chalmers tekniska högskola
Ny serie nr 3586
ISSN 0346-718X

Division of Fluid Dynamics
Department of Applied Mechanics
Chalmers University of Technology
SE-412 96 Göteborg, Sweden

Phone: +46-(0)31-7721000
Fax: +46-(0)31-7723872

Printed at Chalmers Reproservice
Göteborg, Sweden, 2013

Fuel Mixing in Gas-Solid Fluidized Beds:
A Computational and Experimental Study

MEISAM FARZANEH KALOORAZI

Division of Fluid Dynamics
Department of Applied Mechanics
Chalmers University of Technology

Abstract

Fluidized bed technology has been commercially applied over several decades. However there is still a lack of knowledge that can provide a detailed understanding of the combustion process in fluidized-bed furnaces. Understanding of mixing of fuel particles is crucial in order to achieve efficient combustion, while optimizing the number of fuel feeding ports. Thus, it is important to develop tools for reliable design and scale up of fluidized-bed boilers, including modeling from first principles by Computational Fluid Dynamics (CFD).

In fluidized-bed boilers, there is typically a low mass fraction of large fuel particles in an inert bed of finer solids. The extreme size disparity between the two types of particles makes the modeling of the fuel mixing so complex that the conventional Eulerian-Eulerian (E-E) and Eulerian-Lagrangian (E-L) techniques are not able to correctly handle the particulate mixture. Therefore, the main objective of the present work is to develop new numerical strategies, within the E-E and E-L frameworks, so that they would be able to deal with the fuel mixing process.

As for the E-L, our treatment for the problem of fuel mixing includes applying a three-grid method, consisting of a fine, a coarse and a moving grid. The fine grid is employed to resolve the flow of the carrier phase and to treat the small (inert) particles, whereas the coarse grid is used to calculate the drag forces acting on the fuel particles. Furthermore, the moving grid is used in order to correctly calculate the pressure gradient force on the fuel particles.

In an alternative approach, we also propose a tracking technique that is a combination of the E-E and the E-L. The gas and the inert phase are treated as interpenetrating continua and resolved within the E-E framework, whereas the fuel particles are regarded as a discrete phase. The forces acting on a fuel particle are calculated by using the velocity and pressure fields of the inert solid and gas phases.

To investigate the performance of the methodology, several numerical cases are simulated. Using a statistical analysis, preferential po-

sitions and the dispersion coefficient of the fuel particles are obtained under different operating conditions. The detailed information on the motion of the fuel particles obtained from simulations is compared with that from experiments. It is observed that numerical results are in good agreement with the experimental results.

Besides the numerical work, detailed information on the dynamics of the inert particles in bed is obtained using the Particle Image Velocimetry (PIV) technique. Furthermore, a digital image analysis technique is applied to track an illuminated tracer particle in the bed, in an attempt to reproduce the behavior of the fuel particles. The results of the experimental work are presented in the form of the average velocity vectors of the inert and tracer particles. The slip velocity, defined as the velocity difference between the inert and tracer particles, is also presented. Such measurements have not been reported so far in the literature.

Keywords: Fluidization, Eulerian-Lagrangian, Eulerian-Eulerian, Fuel mixing, Numerical Simulation, Particle Image Velocimetry (PIV)

List of Publications

This thesis is based on the following papers:

I M. Farzaneh; S. Sasic; A, E. Almstedt; F. Johnsson; D. Pallarès, A study of fuel particle movement in fluidized beds, *Industrial & Engineering Chemistry Research*, 52(16), 5791-5805, 2013

II M. Farzaneh; S. Sasic; A, E. Almstedt; F. Johnsson; D. Pallarès, A novel multigrid technique for lagrangian modeling of fuel mixing in fluidized beds, *Chemical Engineering Science*, 66 (22), 5628-5637, 2011

III M. Farzaneh; A, E. Almstedt; F. Johnsson; D. Pallarès; S. Sasic, The crucial role of frictional stress models for simulation of bubbling fluidized beds, *Submitted for journal publication*

IV M. Farzaneh; M. Golubev; A, E. Almstedt; F. Johnsson; D. Pallarès; S. Sasic, Experimental and computational study of fuel mixing in fluidized beds, *To be submitted*

Division of work between authors

The respondent was the principal author and investigator in Papers I to III. All the work was done by the respondent and the papers were written by him and reviewed by the co-authors. The theoretical work described in these papers was extensively discussed with the co-authors.

The experimental measurements reported in Paper IV were carried out by the respondent and Maxim Golubev.

Other relevant publications

- M. Farzaneh; S. Sasic; A, E. Almstedt; F. Johnsson; D. Pallarès, A Novel Multigrid Approach for Lagrangian Modeling of Fuel Mixing in Fluidized Beds. *International Conference on Multiphase Flow ICMF 2010*, Tampa, USA.

- M. Farzaneh; A, E. Almstedt; F. Johnsson; D. Pallarès; S. Sasic, Simulation of Fuel Mixing in Fluidized Beds using a Combined Tracking Technique. *Fluidization XIV, 2013*, Noordwijkerhout, The Netherlands.

- M. Farzaneh; A, E. Almstedt; F. Johnsson; D. Pallarès; S. Sasic, Eulerian-Eulerian-Lagrangian Simulation of Fuel Mixing in Fluidized beds. *International Conference on Multiphase Flow ICMF 2013*, Jeju, Korea.

Acknowledgments

I would like to thank everyone who has been involved in this work and everyone who gave me support and encouragement.

First and foremost, I would like to express my deepest appreciation to my supervisor Assoc. Prof. Srdjan Sasic who has not only been a source of enthusiasm and encouragement, but has also been a great friend throughout this work.

My sincere thanks also goes Prof. Alf-Erik Almstedt, Prof. Filip Johnsson and Dr. David Pallarès for the enlightening and stimulating discussions and helpful advices.

I am very grateful to Dr. Valery Chernoray for his help and support during the experimental work.

Special thanks to all the colleagues and staff of the Division of Fluid Dynamics for the pleasant working atmosphere.

The financial support from The Swedish Energy Agency is gratefully acknowledged.

My warmest and deepest gratitude goes to my parents who raised me, supported me, taught me, and loved me.

Nomenclature

Latin symbols

A	area, m^2
$\vec{C}$	peculiar particle velocity, m/s
$\vec{c}$	instantaneous particle velocity, m/s
C_{fuel}	probability density function of presence of particles, m^2
d	diameter, m
D_{cell}	local dispersion coefficient, m^2s^{-1}
$\overline{D_k}$	global dispersion coefficient, m^2s^{-1}
e	restitution coefficient
$\vec{F}$	force, N
f	drag factor, single velocity distribution function, s/m^4
f^2	pair velocity distribution function, s/m^4
f^0	Maxwellian velocity distribution function, s/m^4
$\vec{F}_{Dip}$	drag between solid phases, Nm^{-3}
$\vec{g}$	gravitational acceleration, ms^{-2}
g	radial distribution function
H_0	initial bed height, m
I	moment of inertia, kgm^2
k	unit vector connecting the centers of the two particles
m	mass, kg
n	number density, $1/m^3$
N_{inert}	number of inert particle
N_{ip}	energy dissipation, $Js^{-1}m^3$
N_P	number of times
$\underline{P}$	pressure, Nm^{-2}
$\underline{P_c}$	collisional stress tensor, Nm^2
$\underline{P_f}$	frictional stress tensor, Nm^2
$\underline{P_k}$	kinetic stress tensor, Nm^2
$\vec{q}$	heat flux, $Js^{-1}m^2$
$\vec{r}$	position, m
Re	Reynolds number
$\vec{T}$	torque, Nm
t	time, s

U_0	fluidization velocity, m/s
$\vec{v}$	velocity, m/s
V_{cell}	volume of cell, m^3
V_{fuel}	volume of fuel particle, m^3
V_{inert}	volume of inert particle, m^3
V_p	volume of particle, m^3
Δl	reference displacement, m
Δt	time interval, s

Greek symbols

α_{fuel}	fraction of fuel particle volume
χ	collisional flux
γ	collisional source
μ	viscosity, Pa.s
ω	rotational velocity, s^{-1}
ϕ	perturbation to Maxwellian distribution function
ψ	property of particle
ρ	density, kg/m^3
θ	fluctuation granular energy, m^2s^2
ε	volume fraction
ε_g	volume fraction of gas phase

Subscripts

g	gas
i	phase i
p	particle, phase p
s	solid

Contents

Paper IV

Chapter 1

Introduction

1.1 Motivation

RECENTLY, the increasing level of greenhouse gas emissions combined with the overall rise in fuel prices have raised demands for renewable energy sources such as biomass. Fluidized beds, which use a heated bed of sand-like material fluidized within a rising column of air, have found several industrial applications such as coal and biomass combustion. The popularity of fluidized bed combustion (FBC) is largely due to the technology's fuel flexibility - almost any combustible material, from coal to municipal waste, can be burnt. Fluid-like behavior of particles in a bed allows oxygen to reach the combustible material much more readily and provides more effective chemical reaction and heat transfer. Lower combustion temperature and consequently lower thermal nitric oxide (NO_x) is another great advantage of the fluidized bed combustion over conventional flame combustion (e.g. burning pulverized coal, fuel or natural gas burners). Furthermore, there is a possibility to add limestone in the combustion chamber to reduce sulfur dioxide (SO_2) emissions.

Bubbling fluidized-bed boilers are widely used for combustion of wood-waste fuels, usually delivered as wood chips. The use of biomass in FBC boilers does not necessitate significant pre-processing. It is sufficient for the fuel material to be crushed to a manageable size, the largest particles being a few centimeters in diameter. As shown in Figure 1.1, the fuel particles are fed into the bed of fine particles via fuel feeding points. The fuel is then distributed in the bed by the motion of the bulk phase.

A homogeneous fuel distribution is crucial to ensure excellent mixing of fuel and combustion air while minimizing the excess air ratio and consequently, operational cost. Another important issue regarding

the design of fluidized-bed combustors is the type, position and number of the feeders.

Bubbling fluidized bed boilers use two types of feed systems: over-bed system and under-bed system. As one can see in Figure 1.1, over-bed feeders are simple, reliable and economical, but result in relatively low combustion efficiency. On the other hand, under-bed feeders give high combustion efficiency. However, the design of the under-bed system is complicated and thus, it is expensive and less reliable. Figure 1.2 shows a schematic of a under-bed feeder. A pneumatic system is usually used to inject coal or other fuel particles into the bed (Basu (2006)).

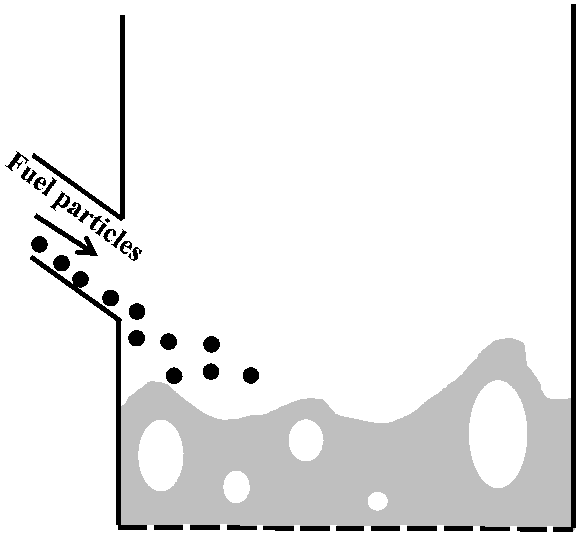

Figure 1.1: Fluidized bed combustor. The fuel enters the combustor through a fuel chute from above the bed

A proper design of the fluidized-bed systems requires sufficient number of fuel feeding points in order to achieve a uniform fuel distribution. A single feeder is adequate for a small boiler having a cross section less that 2 m^2. However, larger beds would need multiple feeding points (Basu (2006)). Therefore, understanding the dispersion of fuel particles is of a great importance to design efficient combustors with optimum number of fuel feeding ports.

Despite the importance of fuel mixing, literature gives limited work on this phenomenon, mostly focused on experiments to estimate a dispersion coefficient (e.g. Highley & Merrick (1971), Xiang *et al.* (1987), Niklasson *et al.* (2002)). However, only experimental calculation of the dispersion coefficient in fluidized beds is not sufficient, because it gives no information on the mechanisms governing the mixing process. Therefore, several studies have been devoted to investigate the detailed

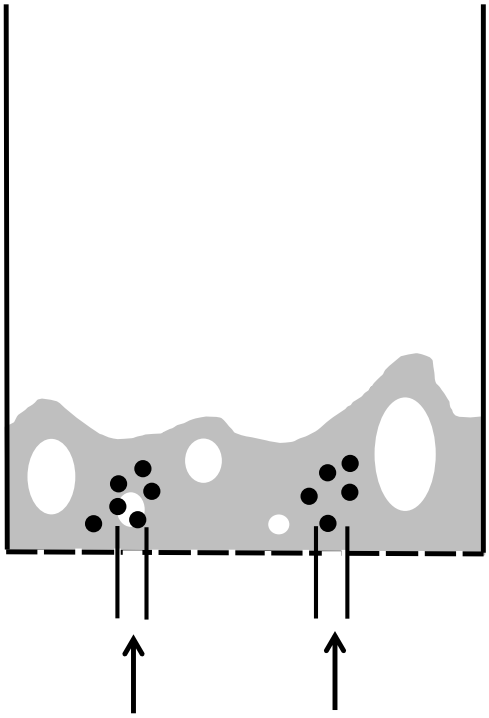

Figure 1.2: Fluidized bed combustor. The fuel enters the combustor from under the bed

motion of fuel particles in fluidized beds. In fluidized-bed boilers, there is typically a low mass fraction of fuel particles (less than 5%) of average size of some 10 mm or more, with a density of 600 to 1000 kg/m^3, in an inert bed of finer solids (less than 1mm) of higher particle density (around 2500 kg/m^3). The differences in size and density between the two types of particles lead to distinctive circulation patterns for the fuel particles in the bed (Agarwal (1987); Lim & Agarwal (1994)).

Nienow *et al.* (1978) studied the motion of various fuel particles (flotsam) immersed in a bulk of small particles (jetsam). They calculated the average rise velocity of the flotsam particles in correlation to the bubble rise velocity. Rios *et al.* (1986) performed a comprehensive study on circulation motion of a single large object in a gas fluidized bed of fine particles. The authors concluded that the position of the large object in the bed depended on the gravity, buoyancy and drag forces. They studied the effect of the density of large spheres and cylinders on their fluidization behavior. Their observations showed that the circulation pattern and penetration of the cylindrical particle into the bed is strongly dependent on the density of the floating object.

In the early stages of fuel mixing studies, experiments mostly in-

cluded various simple visualization techniques. The studies, as indicated above, were typically on the circulatory motion and rising/sinking velocity of a large fuel-like particle in fluidized beds. In addition, they were limited to low fluidization velocities. In a recent work, Pallarès and Johnsson, 2006 used a digital image analysis technique to track a fluorescent fuel-like tracer particle in a bed. The bed material contained glass beads with size and density values similar to those of sand particles typically used in fluidized-bed boilers. Pallarès and Johnsson ran the experiments for 15 minutes and obtained preferential positions, velocity vectors and dispersion coefficients of the tracer under different operating conditions.

In recent years, as a result of rapid development of computational power, the Eulerian-Lagrangian (E-L) or discrete particle methods (DPM) have been employed to model many multiphase flow applications. In the E-L solid particles are tracked individually through the flow domain by solving the Newton′s second law of motion. Tsuji & T. Kawaguchi (1993) were probably the first group using the Lagrangian technique to study fluidization. They simulated a two-dimensional fluidized bed consisting of solid particles of a single size. However, the true advantage of using Lagrangian simulations is its ability to treat cases in which polydispersity exists, such as fuel mixing. The Lagrangian technique was later applied to the modeling of polydisperse suspensions in fluidized beds (Hoomans *et al.* (2000) and Feng *et al.* (2004)), who numerically analyzed mixing and segregation in binary mixtures of particles.

The main problem regarding the E-L technique is that it is computationally demanding and thus still not applicable to large units. As an alternative modeling and simulation tool, the two-fluid (Eulerian-Eulerian) model has often been used to simulate fluidized systems. The Eulerian-Eulerian (E-E) approach treats phases as interpenetrating continua and solves the averaged equations of motion for the particulate phase, together with the governing equations of the gas phase. In terms of computational time, the E-E technique is considerably more affordable than the E-L approach. Most Eulerian models have been limited to solids where particles have the same diameter (Gidaspow (1994); Elwald & Almstedt (1998)). There have been attempts to take into account the size distribution in the E-E approach. (Gidaspow *et al.* (1996); Huilin *et al.* (2001); Iddir & Arastoopour (2005); Fan & Fox (2008)). Nonetheless, because of the narrow size distribution, these models are not suitable for simulation of fuel mixing.

Nearly all the Eulerian and Lagrangian simulations reported in the literature so far deal with particles of same size or with a relatively

small difference in size. However, as mentioned earlier, in the case of combustion in fluidized beds, there is typically a considerable difference between the size of the fuel particles and that of the inert particles. This special feature makes the fuel mixing process so complex that it cannot be handled by the convectional numerical techniques introduced earlier. Therefore, numerical modeling of such a complex system necessitates a special strategy. The main objective of the present is to find methods to overcome the problems arising in the modeling of fuel mixing process. For that purpose suitable approaches are taken, which will be discussed in the next chapter.

Chapter 2

Methodology

In the majority of fluidized bed simulations reported in the literature, the particles are in the same size class meaning that they have a similar size or that the difference between the sizes is small. In addition, as for the numerical simulation of polydisperse mixtures, the volume fraction of each solid phase is comparable to the others. However, the fuel mixing phenomenon has especial features: 1) the properties (size and density) of the fuel particles are substantially different from those of the inert particles, 2) the fuel particles occupy only a few percent of the volume of the bed material. Thus, the traditional numerical techniques, either the Eulerian-Eulerian (E-E) or the Eulerian-Lagrangian (E-L), cannot properly deal with such complexities. To overcome these problems, we introduce suitable modifications within the E-E and E-L frameworks so that they would be able to handle the fuel mixing process. We first look into the issues that prevent the standard E-L and E-E from being able to deal with the fuel mixing phenomenon. Then, we explain in detail our recipe for tackling the problems.

2.1 Conventional Lagrangian Technique

In a typically-used Lagrangian method, single grids are used to resolve the fluid flow and the motion of solid particles. Such an approach yields relatively accurate results when the particles are of similar size. However, when simulating the behavior of fuel particles in a bulk of inert solids, employing a single grid in the simulations will lead to conflicting requirements related to the size of the computational cells. If the size of the cell is chosen based on the size of the fuel particles, the cell will include far too many inert particles (see Figure 2.1) and thereby both the flow of the carrier phase and the motion of the inert particles will not be solved accurately. On the other hand, if the grid is based on the

size of the inert material, the cell size might be smaller than the size of the fuel particles. Thus, there is a need to develop an approach that can deal with mixtures of particles in CFD simulations corresponding to fuel mixing.

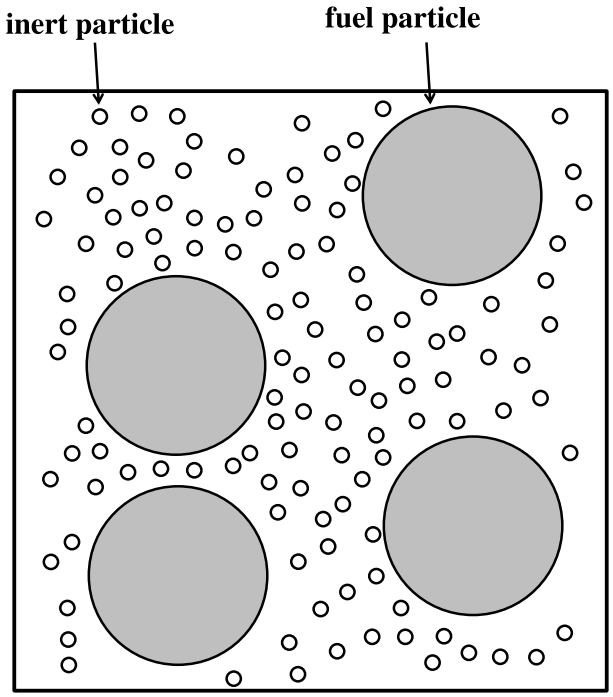

Figure 2.1: A typical grid applied in the conventional Eulerian-Lagrangian approach.

2.2 Conventional Eulerian Technique

The Eulerian-Eulerian (E-E) approach treats phases as interpenetrating continua and solves the averaged equations of motion for the particulate phase, together with the governing equations of the gas phase. The continuity and momentum equations for the gas phase are written as (Syamlal *et al.* (1993)):

$$\frac{\partial}{\partial t}(\varepsilon_g \rho_g) + \nabla \cdot (\varepsilon_g \rho_g \vec{v}_g) = 0, \tag{2.1}$$

$$\frac{\partial}{\partial t}(\varepsilon_g \rho_g \vec{v}_g) + \nabla \cdot (\varepsilon_g \rho_g \vec{v}_g \vec{v}_g) = \nabla \cdot \bar{\bar{S}}_g + \varepsilon_g \rho_g \vec{g} - \sum_{i=1}^{M} \mathrm{I}_{gi} \tag{2.2}$$

where $\bar{\bar{S}}_g$ is the gas-phase stress tensor, I_{gi} is the interaction force

between the gas and the i^{th} solid phase. The i^{th} solids phase mass and momentum balance are as follows:

$$\frac{\partial}{\partial t}(\varepsilon_i \rho_i) + \nabla \cdot (\varepsilon_i \rho_i \vec{v}_i) = 0, \tag{2.3}$$

$$\frac{\partial}{\partial t}(\varepsilon_i \rho_i \vec{v}_i) + \nabla \cdot (\varepsilon_i \rho_i \vec{v}_i \vec{v}_i) = \nabla \cdot \bar{P}_i + \frac{\varepsilon_i \rho_i}{m_i} \vec{F}_{iext} + \sum_{p=1, p \neq i}^{N} \vec{F}_{Dip} \tag{2.4}$$

here ε_i is the i^{th} solids phase volume fraction, ρ_i is the i^{th} solids phase density, $\vec{v}_i$ is the local average velocity of the i^{th} solids phase and $\bar{P}_i$ is the total i^{th} solids phase stress tensor. $\vec{F}_{iext}$ is the external force such as gravitational and gas-solid interaction forces.

The success of an E-E model depends on the proper description of the interfacial forces and the solid stresses (van Wachem *et al.* (2001)). The interfacial forces are used to describe the momentum transfer between the phases, which significantly affects the hydrodynamic behavior of the mixture. The gas-solid drag force has been the subject of many investigations for either mono- or polydisperse suspensions (for example: Wen & Yu (1966); Beetstra *et al.* (2007)).

The drag force between the i^{th} and p^{th} solids phases, $\vec{F}_{Dip}$, is evaluated by the Kinetic theory of Granular Flow (KTGF) which is an analogy with the Chapman-Enskog kinetic theory of gases (Chapman & Cowling (1970)).

The solids stress tensor is composed of three terms as follows:

$$\bar{P} = \bar{P}_{ki} + \bar{P}_{ci} + \bar{P}_{fi} \tag{2.5}$$

here $\bar{P}_{ki}$ and $\bar{P}_{ci}$ are the kinetic and collisional components of the stress tensor respectively. These two terms are calculated using the KTGF. $\bar{P}_{fi}$ is the frictional component of the stress tensor, which becomes activated for highly dense particulate flows. The KTGF can be applied for rapid-flow regimes that are sufficiently dilute, so that interparticle collisions can be assumed instantaneous and binary. However, in highly dense regimes, such as those may be encountered in bubbling fluidized beds, the behavior of the particulate phase is dominated by enduring frictional contacts of multiple neighboring particles. In this so-called quasi-static regime, the fundamental assumptions of the KTGF are violated and the theory may fail to predict the accurate behavior of the system. To overcome this problem, several models were proposed for modeling frictional stresses of dense packed particles (Srivastava & Sundaresan (2003); Jop *et al.* (2006)).

Lun *et al.* (1984) developed a kinetic theory for smooth, inelastic, spherical particles. Their theory accounts for the collision of identical

particles. That approach was later extended to describe binary mixtures (Farrell *et al.* (1986); Jenkins & Mancini (1987)). Iddir & Arastoopour (2005) further extended the theory to a multitype (size and/or density) mixture.

In order to explain the incapability of the KTGF to model the fuel mixing process, we first describe some basic definitions of the theory. The following is adapted from the model developed by Iddir & Arastoopour (2005).

At any time t the number of particles per unit volume n_i and the average value of a property $\psi_i(\vec{c}_i)$ of particulate phase i at space $\vec{r}$ is calculated as follows:

$$n_i(\vec{r},t) = \int f(\vec{c}_i,\vec{r},t)d\vec{c}_i \tag{2.6}$$

$$\langle\psi\rangle = \frac{1}{n_i}\int \psi_i(\vec{c}_i)\, f(\vec{c}_i,\vec{r},t)d\vec{c}_i \tag{2.7}$$

here $f(\vec{c}_i,\vec{r},t)$ is the velocity distribution for particles of species i.

A Boltzmann equation for a multiptype mixture can be expressed as:

$$\frac{\partial f_i}{\partial t} + \frac{\vec{F}_{iext}}{m_i}\cdot\nabla_c f_i + \vec{c}_i\cdot\nabla_r f_i = \sum_{p=1}^{N}\left(\frac{\partial f_{ip}^2}{\partial t}\right)_{coll} \tag{2.8}$$

where m_i is the mass of a particle in the phase i. The right hand side of Equation 2.8 represents the collision between the particles i and p. And f_{ip}^2 is the pair distribution function $f_{ip}^2 = f_{ip}^2(\vec{c}_i,\vec{r}_i;\vec{c}_p,\vec{r}_p)$ defined as the probability of finding two particles i and p such that they are located on $\vec{r}_i$ and $\vec{r}_p$ at time t. The velocities of these particles should be within the range $\vec{c}_i$, $\vec{c}_i + d\vec{c}_i$ and $\vec{c}_p$, $\vec{c}_p + d\vec{c}_p$.

The Boltzmann equation is multiplied by ψ_i and integrated over the velocity field. The resulting equation given below expresses the rate of change of the average value of the property ψ_i because of collision and external force.

$$\begin{aligned}&\frac{\partial}{\partial t}(n_i\langle\psi_i\rangle) + \nabla\cdot(n_i\langle\psi\vec{c}_i\rangle) - \frac{n_i}{m_i}\langle\vec{F}_{iext}\cdot\frac{\partial\psi_i}{\partial\vec{c}_i}\rangle \\ &= \sum_{p=1}^{N}\iiint_{\vec{c}_{ip}\cdot\vec{k}} (\psi_i' - \psi_i)\, f_{ip}^2(\vec{c}_i,\vec{r}_i;\vec{c}_p,\vec{r}_p)d_{ip}^2(\vec{c}_{ip}\cdot\vec{k})d\vec{k}d\vec{c}_i d\vec{c}_p\end{aligned} \tag{2.9}$$

where $\vec{c}_{ip} = \vec{c}_i - \vec{c}_p$ and $d_{ip} = (d_i + d_p)/2$ is the average diameter of the two colliding particles. For illustration, a collision diagram of two

particles is shown in Figure 2.2. $\vec{k}$ is the unit vector connecting the centers of the two particles.

Following Jenkins & Savage (1983), f_{ip}^2 can be expressed as a product of the radial distribution function ($g_{ip}(\varepsilon_i, \varepsilon_p)$) and the single velocity distributions, f_i and f_p:

$$f_{ip}^2\left(\vec{c}_i, \vec{r} - \frac{d_{ip}\vec{k}}{2}; \vec{c}_p, \vec{r} + \frac{d_{ip}\vec{k}}{2}\right) = g_{ip}(\varepsilon_i, \varepsilon_p) \cdot f_i\left(\vec{c}_i, \vec{r} - \frac{d_{ip}\vec{k}}{2}\right) \cdot f_p\left(\vec{c}_p, \vec{r} + \frac{d_{ip}\vec{k}}{2}\right) \tag{2.10}$$

Taking ψ_i to be m_i, $m_i\vec{c}_i$ $1/2(m_i C_i^2)$ yields the continuity, momentum and fluctuating energy equations, respectively. Here $\vec{C}_i$ is the peculiar velocity defined as the difference between the instantaneous and average velocity of the phase i: $\vec{C}_i = \vec{c}_i - \vec{v}_i$

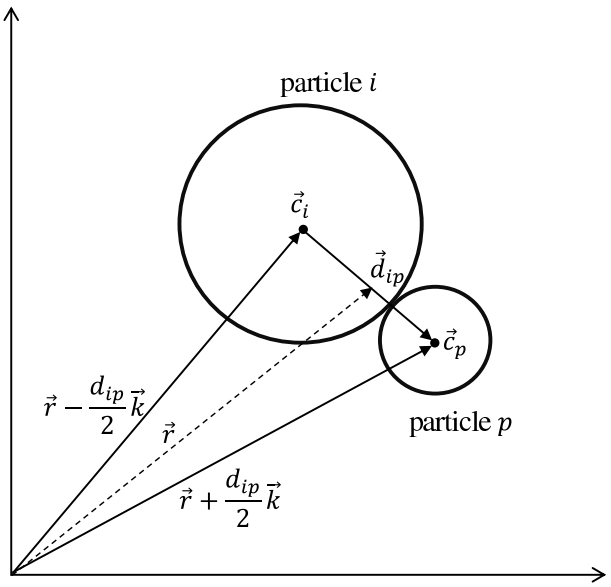

Figure 2.2: Collision of two particles.

In order to solve the collision integral, the postcollisional properties of the particles should be calculated based on the precollisional ones. Following Chapman & Cowling (1970), the balance of momentum of two colliding particles shows that

$$m_o\vec{G} = m_i\vec{c}_i + m_p\vec{c}_p = m_i\vec{c}_i' + m_p\vec{c}_p' \tag{2.11}$$

where $m_o = m_i + m_p$ and $\vec{G}$ is the center of mass velocity. The velocity change during the collision is

$$\vec{c}_i' - \vec{c}_i = -\frac{m_p}{m_o}(1+e)(\vec{k}\cdot\vec{c}_{ip})\vec{k} \tag{2.12}$$

where e is the restitution coefficient of the colliding particles. The translational kinetic energy change during the collision ΔE is

$$\Delta E = \frac{1}{2}\frac{m_i m_p}{m_o}(e^2-1)(\vec{k}\cdot\vec{c}_{ip})^2 \tag{2.13}$$

In order to evaluate the collision integral, it is also required to assume a particle velocity distribution. For this purpose, Iddir & Arastoopour (2005) used the following form:

$$f_i = f_i^0(1+\phi_i) \tag{2.14}$$

where f_i^0 is the Maxwellian velocity distribution

$$f_i^0 = n_i\left(\frac{m_i}{2\pi\theta_i}\right)^{3/2} exp\left[-\frac{m_i C_i^2}{2\theta_i}\right] \tag{2.15}$$

where $\theta_i = \frac{1}{3}m_i\langle\vec{C}_i\cdot\vec{C}_i\rangle$ is the fluctuating energy (granular temperature) of the phase i and ϕ_i is a perturbation to the Maxwellian velocity distribution.

Evaluation of the collision integral for the properties m_i and $m_i\vec{c}_i$ results in the conservation of mass and momentum of the phase i (Equations 2.3 and 2.4).

where the kinetic stress tensor is

$$\bar{P}_{ki} = \rho_i\varepsilon_i\langle\vec{C}_i\vec{C}_i\rangle \tag{2.16}$$

the collisional stress tensor is

$$\bar{P}_{ci} = \chi_{cip}(m_i\vec{c}_i) \tag{2.17}$$

and the collisional momentum source is

$$\vec{F}_{Dip} = \gamma_{cip}(m_i\vec{c}_i) \tag{2.18}$$

where

$$\chi_{cip} = -\frac{-d_{ip}^3}{2}\iiint_{\vec{c}_{ip}\cdot\vec{k}}(\psi_i'-\psi_i)\,f_{ip}^2(\vec{c}_i,\vec{r}_i;\vec{c}_p,\vec{r}_p)\times\vec{k}(\vec{c}_{ip}\cdot\vec{k})d\vec{k}d\vec{c}_i d\vec{c}_p \tag{2.19}$$

$$\gamma_{cip} = -d_{ip}^2\iiint_{\vec{c}_{ip}\cdot\vec{k}}(\psi_i'-\psi_i)\,f_{ip}^2(\vec{c}_i,\vec{r}_i;\vec{c}_p,\vec{r}_p)\times(\vec{c}_{ip}\cdot\vec{k})d\vec{k}d\vec{c}_i d\vec{c}_p \tag{2.20}$$

To close the equations, the fluctuating energy equation is also solved.

$$\frac{3}{2}\frac{\varepsilon_i \rho_i}{m_i}\frac{D\theta_i}{Dt} + \nabla \cdot \vec{q} - \bar{P} : \vec{v}_i = \sum_{p=1}^{N} (N_{ip} - \vec{v}_i \cdot \vec{F}_{Dip}) \tag{2.21}$$

where the heat flux is

$$\vec{q}_i = \rho_i \varepsilon_i \langle \vec{C}_i C_i^2 \rangle + \chi_{cip}(m_i \vec{c}_i^2) \tag{2.22}$$

and collisional energy dissipation is

$$\vec{N}_{ip} = \gamma_{cip}(m_i \vec{c}_i^2) \tag{2.23}$$

The constitutive relations for the stress tensors, heat fluxes, collisional momentum and energy dissipation are given in Iddir & Arastoopour (2005). In the present work, our interest is not to discuss the details of the derivation of these terms. We would instead like to look at the collisional integral for fuel and inert particles.

Figure 2.2 shows a collision of two particles relatively close in size. However, in fuel mixing, the fuel particles are considerably larger that inert particles. The size ratio between the two types of particles is over 20 leading to a substantial mass disparity. As a result, assuming a binary interaction between a fuel and an inert particle (Figure 2.3), according to Equations 2.12 and 2.13, properties cannot be transferred from the small inert to the large fuel particle.

From Figure 2.3 it can be concluded that

$$d_{ip} = \frac{d_i + d_p}{2} \approx d_i \tag{2.24}$$

$$m_o = m_i + m_p \approx m_i \tag{2.25}$$

The above expressions imply that the size and mass of the inert particles will not appear in the relations for the stress tensors, heat fluxes, collisional momentum and energy dissipation. In other words, in those relations, the size and mass of the fuel particles are dominating.

We can also argue that since a fuel particle is surrounded by a number of inert particles as shown in Figure 2.4, even in a relatively dilute particulate flow, the probability of multiple collisions of the inert particles with the fuel particles is high and thus, the inert-fuel particle binary interaction cannot be safely assumed.

Furthermore, the chaos assumption, expressing the absence of the velocity correlation between two colliding particles, is questionable for the mixture shown in Figure 2.4. This is due to the fact that the collision between a large particle and an inert particle tends to be strongly

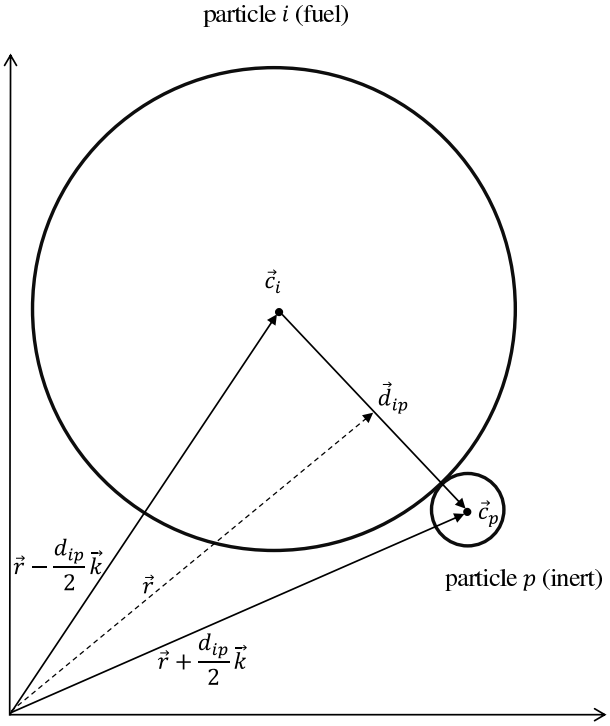

Figure 2.3: Collision between a fuel and an inert particle.

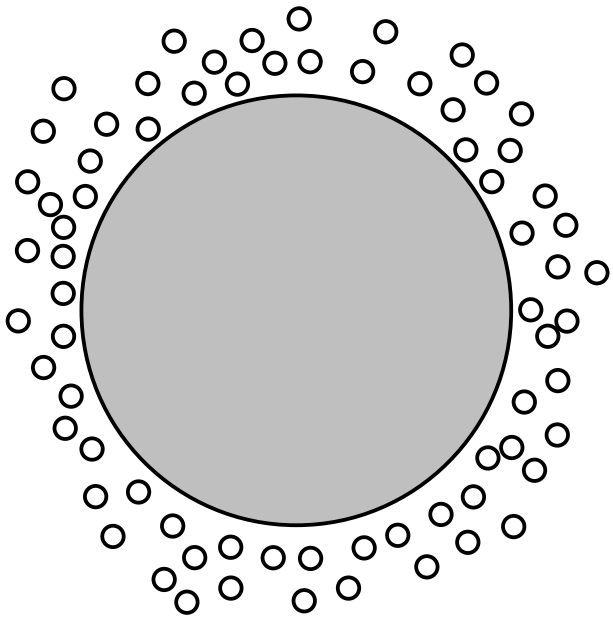

Figure 2.4: A large fuel particles surrounded by small inert particle.

correlated over long times because of a high probability of repeated collisions between the fuel and the inert particle with which it collides

(Sung & Stell (1982)).

To overcome the problems discussed above, we develop two algorithms: 1) a multigrid Lagrangian Technique, which is a modified version of the standard E-L technique, 2) a combined tracking technique, which is a combination of the E-E and the E-L approaches. The detailed explanation of the techniques developed in the present work is given hereafter.

2.3 Multigrid Lagrangian Technique

In the present work we propose a multigrid Lagrangian approach to handle the substantial difference in size between the solid particles in the mixture. The approach uses three grids for the simulations: one coarse, one fine and one that is moving. The fine grid is used to resolve the gas flow field and track the small particles, whereas the drag force on the large particles is calculated using the coarse grid. The moving grid is applied to calculate the pressure gradient force on the fuel particles.

As shown in Figure 2.5, a computational cell of the coarse grid contains a number of cells belonging to the fine grid. The fine grid is used to resolve the gas flow field and to obtain the interaction force between the gas phase and the inert particles. To calculate the drag force on the fuel particles, the volume fraction of the fuel particles is calculated in the coarse grid. Another value required for the drag force calculation is the gas velocity in the coarse cells. This is taken as the averaged velocity of the gas in the small cells included in each large cell. For example, for the large cell shown in Figure 2.5, the velocity of the gas in the center of the large cell is taken as the average value of the velocity of the gas in the 25 small cells. In this approach, the drag force source term due to the presence of the fuel particles in a coarse cell is then equally distributed into the small cells incorporated in the large cell.

Since the fuel particles are substantially larger than the inert particles, a fuel particle will occupy the volume of a number of small cells (Figure 2.6). To calculate the solid volume fraction in the fine grid, the small cells partially or entirely occupied by the fuel particle are first identified and the volume of the fuel particle is then distributed over the cells involved. For instance, the volume of the fuel particle shown in Figure 2.6 is distributed into the cells 1-9. Note that this distribution is proportional to the fraction of the volume of the fuel particle in each cell. The total solid volume fraction (ε_s) in each fine cell is calculated as:

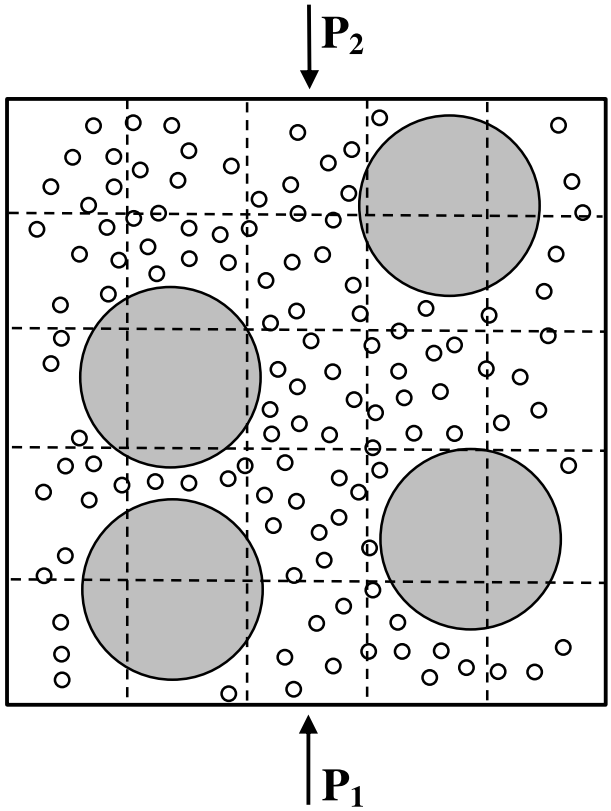

Figure 2.5: Coarse and fine cells applied in the multigrid technique. The fuel and inert particles are in a coarse cell including a number of fine cells.

$$\varepsilon_s = \frac{N_{inert} V_{inert} + \alpha_{fuel} V_{fuel}}{V_{cell}} \tag{2.26}$$

where N_{inert}, V_{inert}, V_{fuel}, V_{cell} and α_{fuel} are the number of inert particles is the fine cell, the volume of a single inert particle, the volume of a single fuel particle, the volume of the fine cell and the fraction of the fuel particle volume within the fine cell, respectively. For a cell completely occupied by a fuel particle (cell No. 5 in Figure 2.6) the carrier phase conservation equations cannot be solved and instead, a constant minimum value ($\varepsilon_{g,low} = 0.05$) for the volume fraction of the continuous phase is applied, as proposed by Darmana *et al.* (2005) for tracking bubbles in a liquid.

An important force acting on a solid particle is the pressure gradient or buoyancy force, especially for the light and large fuel particles simulated here. In a Lagrangian framework, the pressure gradient force is calculated as:

$$F_B = (P_1 - P_2)A\frac{V_p}{V_{cell}} \tag{2.27}$$

As seen in the Figure 2.5, P_1, P_2, A and V_p are the pressure on the south and north face of the cell, the surface area of the face and the particle volume, respectively.

The method described above was first applied to calculate the pressure gradient force on the fuel particles by using the coarse grid shown in Figure 2.5. This approach yielded some un-physical behavior, where the fuel particles did not circulate in the bed but stayed all the time in the near-wall regions. We argue that this behavior was caused by the size of the coarse grid. The coarse grid applied here is so large that it cannot accurately capture the complex pattern of the flow around the fuel particles in a cell. This consequently leads to a less accurate calculation of the pressure field. Therefore, in addition to the coarse and fine grids, we applied an additional moving grid to calculate the pressure gradient force on the fuel particles. The moving cells are created around the fuel particles and their size is equal to the diameter of the fuel particles as shown in Figure 2.6). The pressure values on the faces of the moving cells are obtained from the values on the fine grid using a bilinear interpolation.

2.3.1 Fluidized Bed Scaling

Numerical results of the Lagrangian simulations are compared with the experimental data given by Pallarès & Johnsson (2006), who studied mixing mechanisms of fuel particles in narrow two-dimensional ($0.4\text{m} \times 2.15\text{m} \times 0.015\text{m}$) fluidized beds. A schematic view of the setup is shown in Figure 2.7

Pallarès and Johnsson used a digital image analysis technique to track a phosphorescent tracer particle. Glass beads with an average size of $330\mu\text{m}$ and density of 2500kg/m^3 were used as the inert bed material. The properties of the tracer particles were chosen so that the size and density ratios between the tracer and inert solids resembled that of fuel particles in a fluidized-bed combustor. In addition to the results presented in the above mentioned works, other measurements have been carried out in order to extract new results needed for the comparison.

It was not possible in this thesis to exactly model the conditions applied by Pallarès & Johnsson (2006), since this would result in a too large number of inert particles to carry out Lagrangian simulations. Thus, the properties of the simulated bed are chosen in such a way to secure reasonable simulation times while obtaining results relevant for

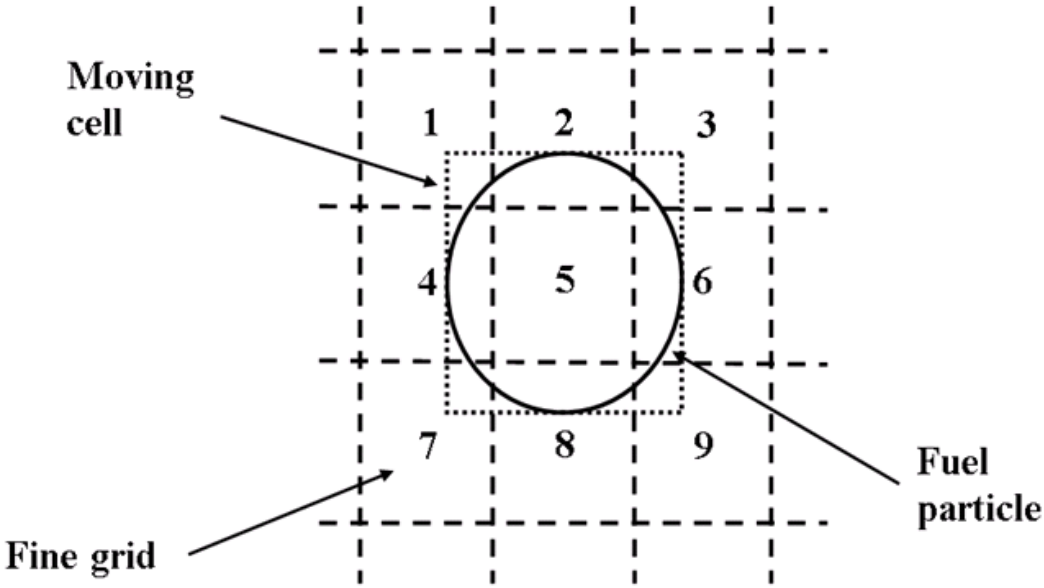

Figure 2.6: Schematic description of the fine grid and a moving cell for determination of the pressure gradient force. Cell 5 is completely blocked by a fuel particle.

comparison with experiments. The experimental beds are scaled using the simplified scaling laws for fluidized beds, suggested by Glicksman *et al.* (1993). As a result of the scaling, new properties for the inert bed material and the gas flow are obtained.

2.3.2 Equations of Particle Motion

The multigrid technique has been implemented into the MFIX (Multiphase Flow with Interphase eXchange), which is an open source computer code developed at the National Energy Technology Laboratory (NETL) for describing the hydrodynamics, heat transfer and chemical reactions in fluid-solids systems (https://mfix.netl.doe.gov). When using the Lagrangian approach, all the particles are tracked individually and the equations of translational and rotational motion of the particles are solved. The fluid-particle interaction force, the gravitational force and the particle-particle collisional force are taken into account. The equations of motion of a particle are

$$\vec{\dot{r}} = \frac{\vec{F}}{m} + \vec{g} \tag{2.28}$$

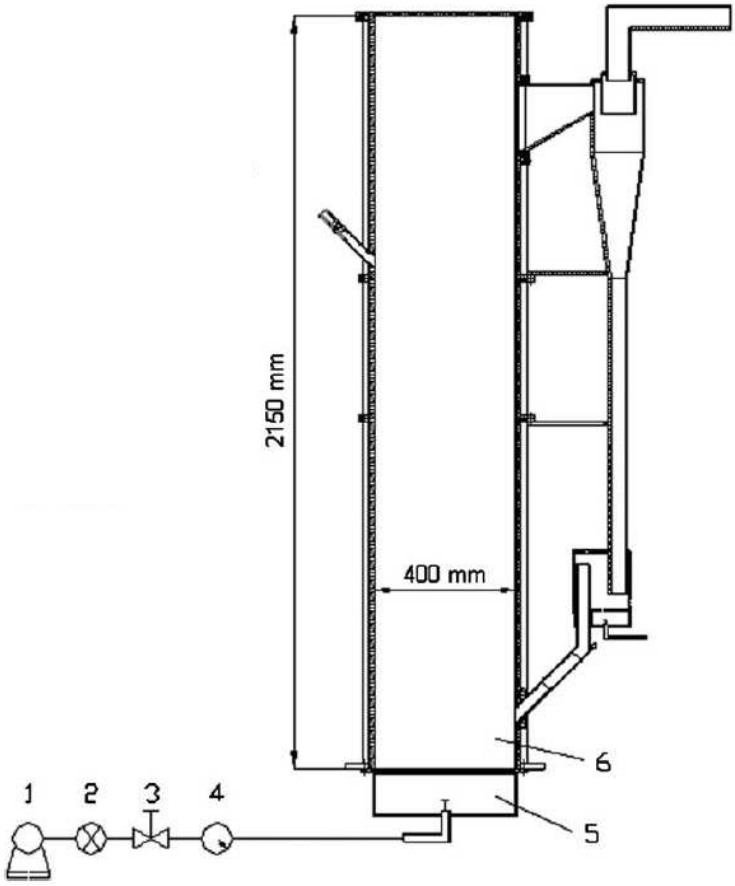

Figure 2.7: Schematic of the fluidized bed setup by Pallarès & Johnsson (2006): 1) Compressor, 2) stop valve, 3) control valve, 4) rotameter 5) plenum, 6) riser. The bed is numerically modeled in the present work

$$\dot{\vec{\omega}} = \frac{\vec{T}}{I} \tag{2.29}$$

where $\vec{r}$ is the particle position vector, m is the particle mass, $\vec{g}$ is the gravitational acceleration, $\vec{\omega}$ is the rotational velocity, I is the moment of inertia of particles. $\vec{T}$ is the torque caused by contact forces, and $\vec{F}$ is the force acting on the particles consisting of the fluid-particle interaction force, the pressure gradient force, and the particle-particle collision force. These forces are discussed in detail in the appended papers.

2.3.3 Examples of Results

To investigate the capability of the multigrid technique to model fuel mixing in fluidized beds, a number of operating conditions relevant for fluidized-bed boilers are modeled numerically in this thesis. A statistical analysis is conducted to study the movement of the fuel particles and capture their distribution in the bed. As a result, their preferential positions are obtained using the probability density function (PDF) of the presence of the fuel particles. The average velocity vectors of the fuel particles are also calculated. In addition, the dispersion coefficient of the fuel particles for the bed in each statistical cell is evaluated.

The computational results are compared with available experimental data by Pallarès & Johnsson (2006) and Pallarès *et al.* (2007). It is shown that the conventional single-grid Lagrangian method is not able to capture complexity of the bed pattern. However, the new multigrid technique developed in the present work significantly improves the results. A few examples of the results for a case ($H_0 = 0.4$m and $U_0 = 0.4$m/s) are given below. Detailed studies can be found in Papers I and II.

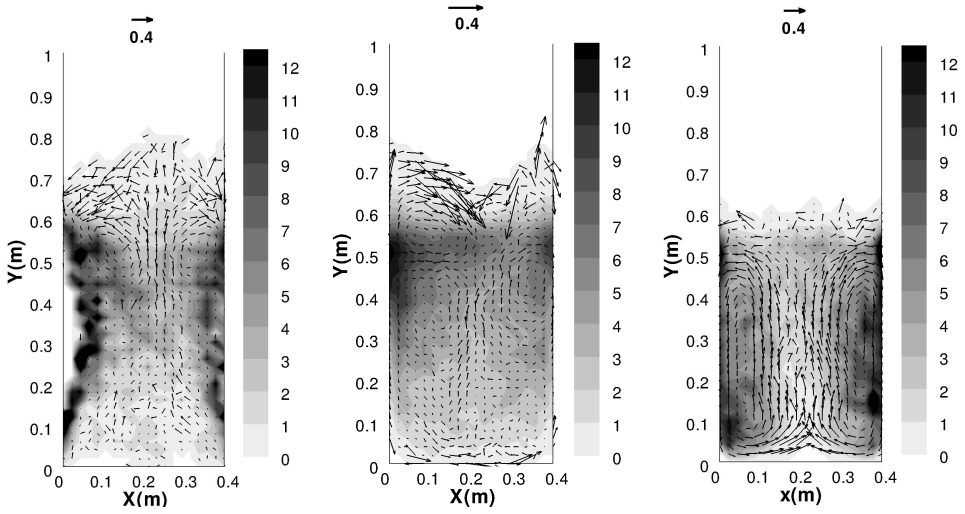

Figure 2.8: Tracer particle velocity and probability density function of the presence of tracer particles: a) experiments by Pallarès & Johnsson (2006); b) single-grid simulations; c) multigrid simulations

Figures 2.8 and 2.9 give a comparison between the computational results of a fluidized bed and the corresponding experimental results for the concentration and average velocity vectors of the fuel particles (Figure 2.8) and expressed as the local horizontal dispersion coefficient

(Figure 2.9). The experimental results in Figure 2.8(a) show that a tracer particle tends to spend a significant fraction of time in the near-wall regions of the bed, represented by two large dark regions. As can be seen here, Overall the the average movement of the tracer particle forms two large vortices.

Figure 2.8(b) illustrates that the single-grid simulations give an overall picture relatively similar to the experiments with respect to where the fuel particles appear. Yet, the clear vortex structure of the experiments is not captured by the single-grid simulations. Instead, the multigrid approach, Figure 2.8(c), accurately reveals two large vortices not present in the simulations when using the single-grid method. The general behavior of the fuel particles obtained from the numerical simulations with the multigrid approach agrees well with the experimental observations.

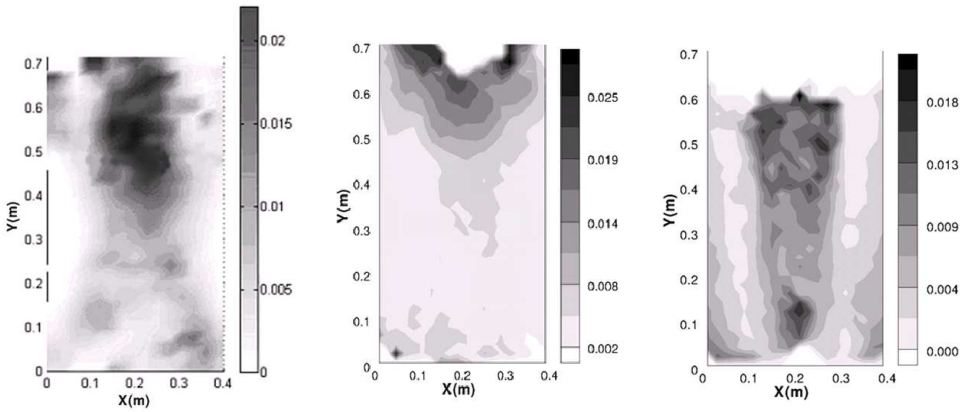

(a) (b) (c)

Figure 2.9: The tracer particle velocity and probability density function of the presence of tracer particles: a) experiments by Pallarès & Johnsson (2006); b) single-grid simulations; c) multigrid simulations

The inability of the single-grid simulations to capture the complex pattern of the fuel particles is also illustrated by the distribution of the local horizontal dispersion coefficient. According to the experimental results, Figure 2.9(a), there is a high-dispersion region stretched along the height of the bed. This region representing the main bubble path is shown as a long dark area. The high-dispersion region is not well detected by the single-grid modeling (Figure 2.9(b)). However, the multigrid modeling captures the preferred bubble path and high-dispersion region in good agreement with the experimental observations (Figure 2.9(c)).

2.3.4 Distributor Modeling

A uniform velocity profile has been a common choice as the inlet boundary condition in the majority of the simulations reported in the literature. Such a boundary condition corresponds to a situation in which the pressure drop over a distributor is much higher than that over the bed. In such simulations, the fluidized bed and its air supply system are assumed independent and the possible influence of the air-plenum to fluid dynamics of the bed is thus neglected. However, the situation is different for fluidized beds with a low pressure drop distributor, as is the case in most industrial applications due to a need to reduce the cost of fan power. It has been shown before that the pressure drop over the air distributor, which determines the uniformity of the inflow, has a great influence on the characteristics of the bed (Svensson *et al.* (1996); Peirano *et al.* (2002); Sasic *et al.* (2006)). To study the influence of the distributor boundary condition, an integrated system consisting of a bed and a plenum is computationally examined and the results are compared with those when the uniform velocity profile is assumed at the air distributor.

In the current work, to accurately formulate the inlet boundary condition, the plenum is included in the computational domain and the air distributor is modeled as a porous zone with a specified resistance (Figure 2.10). Furthermore, the numerical results using this boundary condition are compared with those using the uniform velocity imposed at the distributor. In is concluded that inclusion of the air-supply system in the computational domain is essential for modelling low-pressure-drop distributors, where the hydrodynamics of the bed is coupled with the flow field inside the plenum. The results of the comparison are given in Paper II.

2.4 Combined Tracking Technique

Although the E-L technique is straightforward and it gives detailed information on the dynamics of the particulate systems, it requires significant computational time. Therefore the Eulerian-Eulerian (E-E) has often been the preferred approach to simulate large scale fluidized systems. In terms of computational time, the E-E technique is considerably more affordable than the E-L approach and thus, in this thesis we choose this technique to formulate a methodology for studying the behavior of fuel particles in fluidized beds. We propose a combined tracking technique that we term the Eulerian-Eulerian-Lagrangian (E-E-L) technique. The inert phase is composed of a large number of sand-like

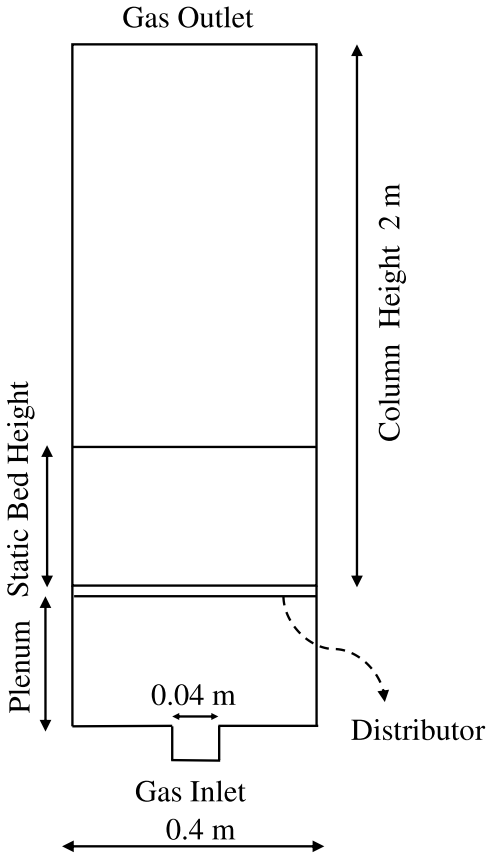

Figure 2.10: Fluidized beds simulated in the present work with the plenum included in the computational domain

small particles and is treated as a continuous phase. The forces acting on a fuel particle, e.g. the drag and buoyancy, are calculated by using the velocity and pressure fields of the inert solid and gas phases. A limited number of large fuel particles are tracked using a Lagrangian particle tracking method.

The equation of motion of the fuel particles is written as:

$$m_{fuel}\frac{d\vec{v}_{fuel}}{dt} = 3d_{fuel}\mu_g f_g(\vec{v}_g - \vec{v}_{fuel}) + 3d_p\mu_s f_{s0}(\vec{v}_s - \vec{v}_{fuel}) + m_p\vec{g} - \rho_{\text{mix}}\vec{g}V_{fuel} \tag{2.30}$$

where $\vec{v}_g$ and $\vec{v}_s$ are the velocity of the gas and the inert solid phases. Also, $\vec{v}_{fuel}$, m_{fuel}, d_{fuel}, V_{fuel} are the velocity, mass, diameter and volume of a fuel particle, respectively.

We calculate the drag force on the fuel particle from the other two phases in an independent manner. In Equation 2.30, the first and second terms on the r.h.s represent the drag forces on the fuel particles

exerted by the gas and inert solids phases. The third term is the weight of the fuel particle and the last term is the buoyancy force exerted by the mixture (gas and inert solids).

The density of the mixture of gas and inert solids is calculated as follows:

$$\rho_{\text{mix}} = \varepsilon_s \rho_s + \varepsilon_g \rho_g \tag{2.31}$$

The drag factor on a fuel particle exerted by the gas phase is expressed by the correlation proposed by Wen & Yu (1966), which takes into account the effects of the local volume fraction of the gas phase:

$$f_g = \varepsilon_s^{-3.7} f_{g0} \tag{2.32}$$

The drag factors on an isolated fuel particle exerted by the inert and gas phases, f_{s0} and f_{g0}, are calculated by the well-established correlation (Equations 2.33 and 2.34) proposed by Schiller & Nauman (1933) for particle Reynolds numbers of up to 1000. This correlation is still extensively used for calculation of drag force on spheres (Crowe *et al.* (1998)).

$$f_{s0} = (1 + 0.15\text{Re}_s^{0.697}) \tag{2.33}$$

$$f_{g0} = (1 + 0.15\text{Re}_g^{0.697}) \tag{2.34}$$

The particle Reynolds numbers:

$$\text{Re}_g = \frac{\rho_g d_{fuel} |\mathbf{v}_g - \mathbf{v}_{fuel}|}{\mu_g} \tag{2.35}$$

$$\text{Re}_s = \frac{\rho_s d_{fuel} |\mathbf{v}_s - \mathbf{v}_{fuel}|}{\mu_s} \tag{2.36}$$

2.4.1 Frictional Stress Models

As indicated in Equation 2.30, the movement of the fuel particles is strongly governed by the dynamics of the inert solid and gas phases. Therefore, an accurate modeling of the inert particulate phase is crucial in order to correctly describe the behavior of the fuel particles. The choice of different E-E models is expected to have a significant impact on the hydrodynamics of the bed (van Wachem *et al.* (2001); Passalacqua & Marmo (2009)) and consequently on the movement of the fuel particles. Hence, a special focus is placed on the selection of an appropriate formulation of an E-E model.

The E-E approach uses KTGF to model the stresses of the solid phase (Lun *et al.* (1984)) for adequately dilute regimes, where inter-particle collisions can be assumed instantaneous and binary. However, in highly dense regimes, the dynamics of the particulate flow is governed by sustained frictional contacts of multiple neighboring particles. In such a regime the KTGF is not reliable and new frictional models are required. For this purpose, several models, mostly derived from the critical state theory of soil mechanics, have been proposed for calculation of frictional stresses ($\bar{P}_{fi}$ in Equation 2.5) of dense packed particles (Schaeffer (1987); Srivastava & Sundaresan (2003)). These models have traditionally been used to model dense particulate systems related to fluidization.

In the present work we have found that the mechanical behavior of dense particulate assemblies is of such complexity that the soil mechanics alone cannot deal with it and that modeling of such a system requires a more comprehensive theory. Therefore, another frictional stress model recently proposed by Jop *et al.* (2006) is implemented into the MFIX code. This model was proposed by identifying similarities between the behavior of granular materials and that of visco-plastic fluids. We conclude that the use of the model suggested by Jop *et al.* (2006) leads to a more correct prediction of the bed hydrodynamics.

2.4.2 Examples of Results

To examine the performance of the frictional stresses, we analyze the motion of a single fuel particle in the bed by looking at the experimental and numerical results for its position and velocity. The results for a case ($H_0 = 0.4$m and $U_0 = 0.4$m/s) are presented below.

Figure 2.11 shows the vertical position of the fuel particle for a period of 100 seconds of operation. The experimental result shown in Figure 2.11(a) illustrates that the fuel particle moves in a cyclic pattern. It moves downwards at the regions near the walls. Then, close to the distributor, it starts moving upwards with the upcoming bubbles and returns to the surface. As seen here, the fuel particle spends most of the time in the sinking (descending) phase, whereas the rising (ascending) one takes a much shorter time.

Figure 2.11(b) shows the motion of the fuel particle simulated using the frictional model proposed by Schaeffer (1987). This model captures the circulation of the fuel particle, but it clearly predicts much shorter cycles. The result of the model of Srivastava & Sundaresan (2003) shown in Figure 2.11(c) does not give significant change compared to the results of the model of Schaeffer (1987).

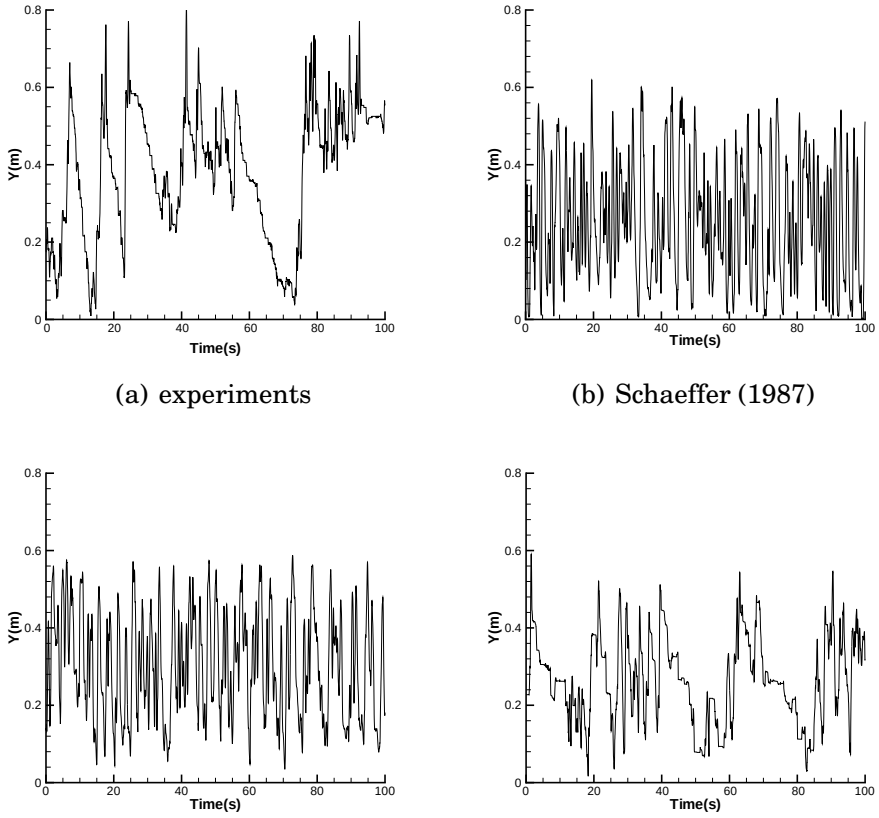

(a) experiments (b) Schaeffer (1987)

(c) Srivastava & Sundaresan (2003) (d) Jop *et al.* (2006)

Figure 2.11: The vertical position of the fuel (tracer) particle: a comparison between experimental observations and numerical results obtained using different frictional stress models.

Employment of the model developed by Jop *et al.* (2006) (Figure 2.11(d)), however, results in a circulation pattern for the fuel particle that is more similar to the experimental results. Here, the fuel particle sinks rather slowly. These slow-moving periods represent situations in which the fuel particle is surrounded by the inert particles and therefore, it totally follows the motion of the inert phase. The better prediction obtained by the model of Jop *et al.* (2006) can be explained by the fact that this model gives higher solids viscosity, and consequently, lower solids velocity in the dense particulate flow. In dense regimes, the frictional stresses play a major role. It is concluded that the model proposed by Jop *et al.* (2006) can better take into account the friction between the particles, and thus the stresses in the particulate phase, compared to the other two models. The detailed description of the models and the more computational results are found in Paper III and IV.

Chapter 3

Experiments

DISTRIBUTION of the fuel particles in a bed is strongly governed by the dynamics of the inert solid phase. Therefore, having information on the motion of the inert particles would be of great use to achieve a better understanding of the fuel particles movement pattern. For this purpose, we have performed measurements using the Particle Image Velocimetry (PIV) technique to obtain detailed information on the dynamics of the inert particles in fluidized beds.

PIV is a non-intrusive experimental method to obtain instantaneous flow patterns of a system. It was originally developed to study flows in liquid or liquid-gas systems (Adrian (2005)). In traditional PIV measurements, tracer particles are released inside the flow and they have to be illuminated in a plane of the flow at least twice within a short time interval. As a result, the displacement of the particle images is determined through evaluation of the PIV recordings.

Recently, the PIV technique was adapted for use in gas-solids flows such as fluidized beds (Mü1ller *et al.* (2007)). Here, there is no need for tracer particles, because the particles themselves can be tracked. Note that since fluidized beds are opaque, due to presence of solid particles, PIV measurements of such systems are limited to thin (two-dimensional) units.

In Paper III, the results of numerical simulations are compared with experimental observations of Pallarès & Johnsson (2006). Pallarès & Johnsson (2006) presented their results for the trajectory of a single fuel-like tracer particles and they gave no information on the inert particulate phase. We numerically track a tracer particle using the combined tracking technique and compare the motion of the tracer with that obtained from the experiments. By looking at the tracer movement pattern, we investigated the performance of frictional stress models for the inert particles (It was briefly discussed in the previous chapter in sections 2.4.1 and 2.4.2). We argue that the motion of the fuel par-

ticles would principally be governed by what happens with the inert particles, especially in the dense regions of the bed. However, even though this was a fairly reasonable assumption, to gain confidence in the numerical methodology, more direct experimental information on the inert particulate phase in a bed is needed. Therefore, we use the PIV technique in order to obtain more information on the flow field of the inert particles. In this way, we will provide sufficient and suitable experimental data to validate the results of our numerical simulations. To perform the experimental work, the fluidized-bed unit previously manufactured and tested by Pallarès & Johnsson (2006) (Figure 2.7) with minor modifications is used.

In addition to the PIV measurements, a digital image analysis technique is applied to track an illuminated tracer particle in the bed, in an attempt to reproduce the behavior of the fuel particles.

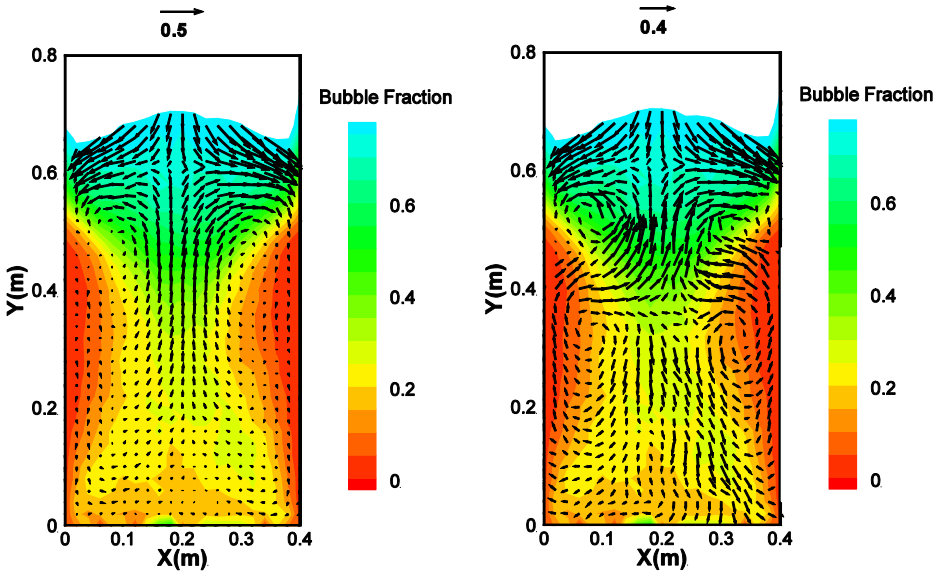

(a) Inert solids circulation (b) Slip velocity

Figure 3.1: The bubble fraction, the circulation pattern of inert solids and the slip velocity in the bed obtained by the experiments.

The results of the experimental work in the form of the average velocity vectors of the inert and tracer particles are obtained. The slip velocity, defined as the velocity difference between the inert and tracer particles, is also calculated. The slip velocity could be an indication of the interaction between the tracer/inert particles and bubbles in a bed.

Figure 3.1(a) shows the bubble fraction and the averaged velocity vectors of the inert solids for an experimental case ($H_0 = 0.4$m and $U_0 = 0.9$m/s). As seen in the figure, the movement of the inert parti-

cles exhibits two vortices. Figure 3.1(a) shows that bubbles are created near the walls and then detach and rise. The bubbles coalesce at the center of the bed and form a larger bubble. The upcoming bubbles carry the inert particles to the bed surface. The inert particles then slowly descend near the walls.

Figure 3.1(b) shows the slip velocity in the bed. As observed here, the slip velocity is directed downwards in the main bubble path. It means that the velocity of the inert particles is lower than that of the fuel particles in this region. This is due to the fact that the rising bubbles carry the tracer upwards, while the inert particles drift down in the wake of the bubbles. Even though there are always some inert particles that ascend with the bubbles, the velocity of the inert particles is, in average, much lower than that of the tracer. On the other hand, in the dense regions (near the walls) the slip velocity is small, implying that the tracer particle sinks together with the emulsion phase. This is can be explained by the fact that the tracer is most of the time submerged in the inert phase particles.

According to our knowledge, such experimental studies on both inert and fuel particles have not been reported in the literature. Details of the experimental setup and more results are presented in Paper IV.

Chapter 4

Concluding Remarks

FUEL MIXING in fluidized beds is investigated by studying the movement of a limited number of large fuel particles suspended in a bulk of small inert particles. Due to a large difference in size between the two types of particles, the conventional Eulerian-Eulerian (E-E) and Eulerian-Lagrangian (E-L) numerical techniques are not able to correctly simulate that process. Hence, in order to deal with the specific features related to fuel mixing, we propose modifications within both the E-E and E-L.

When it comes to the E-L simulations, we propose a multigrid Lagrangian particle tracking technique, which treats the fuel and inert particles in different grids. A fine grid is employed to resolve the flow of the carrier phase and to treat the small (inert) particles, whereas a coarse grid is used to calculate the drag forces acting on the fuel particles. Furthermore, a moving grid is used in order to correctly calculate the pressure gradient force on the fuel particles

At present, the computational cost of the E-L simulations is still prohibitive to employ the the technique for simulating large-scale units. For this reason, we develop in this work a tracking technique that is a combination of the E-E and the E-L simulation frameworks. The technique treats the bulk phase of inert particles as a continuum and solves the averaged equations of motion for the inert particles, together with equations resolving the flow of the gas phase. The combined technique then tracks the fuel particles as a discrete phase.

This is a summary of the main results:

Multigrid Lagrangian Technique: Preferential positions, velocity vectors and the dispersion coefficient of the fuel particles are obtained and compared with experiments. The results are obtained using both the conventional single-grid and the proposed multigrid techniques. It

is demonstrated that the multigrid methodology considerably improves the results.

Combined Tracking Technique: In addition to the results of preferential positions, velocity vectors and the dispersion coefficient, detailed information on the trajectory and velocity of fuel particles is obtained. The results show that the circulatory motion of the fuel particles is well captured by the numerical simulations and the computational results are in good overall agreement with experiments. The setup of the E-E technique and, in particular, the representation of a frictional stress tensor, has a major influence on the performance of the technique. It is shown that the use of the model recently suggested by Jop *et al.* (2006) leads to a more correct prediction of the movement of the fuel particles in the bed, in comparison to the commonly-used frictional models of Schaeffer (1987) or Srivastava & Sundaresan (2003).

Measurements: We use Particle Image Velocimetry (PIV), together with a digital image analysis, to get more insight into the motion of the inert and fuel particles in a bed. We obtain detailed information on the dynamics of the two types of particles and the interaction between them. Moreover, the experiments illustrate how the movement of the particles are influenced by the bubble movement pattern in the bed. In the regions rich in bubbles, the fuel particles is less affected by the inert particles. On the other hand, in the dense particulate regions, the fuel particles almost completely follow the emulsion phase.

4.1 Future work

The present thesis is a step forward in understanding the process of fuel mixing in fluidized-bed combustors. The numerical models developed in both the Eulerian-Lagrangian and Eulerian-Eulerian approaches can well mimic the dynamics of fuel particles. In addition, PIV measurements present new information on fuel mixing and interaction between the fuel and inert particles in fluidized beds. However, there is still a lot to learn on the process of fuel mixing in fluidized beds. For further research within this subject, both the numerical and experimental techniques can be improved. The following suggestions are made for future research on fuel mixing in fluidized beds:

Eulerian-Lagrangian Technique: Lagrangian particle tracking technique is straightforward to implement and it gives detailed information

on the motion of individual particles in a bed. Thus, it should be a preferred choice for modeling particulate flows, such as fluidization. The main problem regarding the E-L technique is that it is computationally demanding and thus still not applicable to large units. Therefore, in the present work, we use the scaling laws to reduce the number of inert particles, which could be handled by the currently available computational power. However, by constantly increasing the latter and, together with new parallelization algorithms, there will be possibilities to simulate large-scale fluidized beds with less simplification. In addition, in fluidized bed combustors, due to chemical reactions, the size and density of the fuel particles change. In the present work, a cold fluidized bed is modeled and the fuel particles are assumed non-reactive and thus, their properties do not change. Fuel particles with varying properties might have different dynamics from those in the cold bed. Hence, to accurately model the behavior of fuel particles under operating conditions, the change of their properties should be taken into account.

Eulerian-Eulerian Technique: In the present work, we combine the E-E and the E-L to track fuel particles by solving the Newton′s second law of motion. The drag, gravitational and buoyancy forces are taken into account. Other forces such as the added mass could also be included. The changes in the size and density of the fuel particles could also be added to the tracking technique. We observe in the thesis that the effect of the frictional stress models on the hydrodynamics of the bed and consequently, on the movement of the fuel particles is significant. Even though the visco-plastic model of Jop *et al.* (2006) can better estimate the frictional stresses in dense particulate flows compared with the other conventional models, there is still room for further improvements of the available models. For example, particle properties, such as frictional and restitution coefficients, play no role in the formulation of the proposed frictional stress models. We believe there is a correlation between the particle properties and the frictional stresses that could be a subject of future studies.

Measurements: In this thesis, we had to restrict to using two low-frequency cameras, taking two subsequent images with a short inter-frame time. The drawback of this process is that the adjustment of the two cameras (in order for them to take exactly the same images) is a very cumbersome task. There is always some error, especially for cases with low fluidization velocity. Therefore, in order to perform more accurate experiments, a high speed camera will be required for future

experimental studies. In addition, modifications should be made on the experimental apparatus and the illumination setup in order to obtain the local concentration of the particulate phase (using the current setup such measurements are not possible). By means of such measurements in combination with simulations, new correlations for calculation of the forces (i.e. the drag) on a fuel particle could be achieved. The solids volume fraction plays a major role on the forces acting on the fuel particles.

Bibliography

ADRIAN, R. J. 2005 Twenty years of particle image velocimetry. *Experiments in Fluids* **39**, 159–169.

AGARWAL, P. K. 1987 The residence phase of active particles in fluidized beds of smaller inert particles. *Chemical Engineering Science* **42**, 2481–2483.

BASU, P. 2006 *Combustion and Gasification in Fluidized beds*, 1st edn. CRC Press.

BEETSTRA, R., VAN DER HOEF, M. A. & KUIPERS, J. A. M. 2007 Drag force of intermediate reynolds number flow past mono- and bidisperse arrays of spheres. *AIChE Journal* **53**, 489–501.

CHAPMAN, S. & COWLING, T. G. 1970 *The Mathematical Theory of Non-uniform Gases*. Cambridge University Press,.

CROWE, C. T., SOMMERFELD, M. & TSUJI, Y. 1998 *Multiphase Flows with Droplets and Particles*. CRC Press, Boca Raton, FL.

DARMANA, D., DEEN, N. G. & M.KUIPERS, J. A. 2005 Detailed modeling of hydrodynamics, mass transfer and chemical reactions in a bubble column using a discrete bubble model **60**, 2283–3404.

ELWALD, H. & ALMSTEDT, A. E. 1998 Fluid dynamics of a pressurized fluidized bed: comparison between numerical solutions from two-fluid models and experimental results. *Chemical Engineering Science* **54**, 329–342.

FAN, R. & FOX, R. O. 2008 Segregation in polydisperse fluidized beds:validation of a multi-fluid model. *Chemical Engineering Science* **63**, 272–285.

FARRELL, M., LUN, C. K. K. & SAVAGE, S. B. 1986 A simple kinetic theory for granular flow of binary mixtures of smooth, inelastic, spherical particles. *Acta Mechanica* **63**, 45–60.

FENG, Y. Q., XU, B. H., ZHANG, S. J., YU, A. B. & ZULLI, P. 2004 Granular dynamics simulation of segregation phenomena in bubbling gas-fluidised beds. *AIChE* **50**, 1713–1728.

GIDASPOW, D. 1994 *Multiphase Flow and Fluidization: Continuum and Kinetic Theory Descriptions*. Academic Press Inc, Boston.

GIDASPOW, D., HUILIN, L. & MANGER, E. 1996 Kinetic theory of multiphase flow and fluidization: Validation and extension to binaries. XIXth International Congress of Theoretical and Applied Mechanics, Japan.

GLICKSMAN, L. R., HYRE, M. & WOLOSHUN, K. 1993 Simplified scaling relationships for fluidized beds. *Powder Technology* **77**, 177–199.

HIGHLEY, J. & MERRICK, D. 1971 The effects of the spacing between solid feed points on the performance of a large fluidized bed reactor. *A.I.Ch.E. Symposium Series* **67**, 219–227.

HOOMANS, B. P. B., KUIPERS, J. A. M. & VAN SWAAIJ, W. P. M. 2000 Granular dynamics simulation of segregation phenomena in bubbling gas-fluidised beds. *Powder Technology* **109**, 41–48.

HUILIN, L., GIDASPOW, D. & MANGER, E. 2001 Kinetic theory of fluidized binary granular mixtures. *Physical Review E* **64**, 61301–61319.

IDDIR, H. & ARASTOOPOUR, H. 2005 Modeling of multitype particle flow using the kinetic theory approach. *AIChE Journal* **51**, 1620–1632.

JENKINS, J. T. & MANCINI, F. 1987 Balance laws and constitutive relations for plane flows of a dense, binary, mixture of smooth, nearly elastic, circular disks. *J. Appl. Mech.* **64**, 27–34.

JENKINS, J. T. & SAVAGE, S. B. 1983 A theory for the rapid flow of identical, smooth, nearly elastic, spherical particles. *J Fluid Mech* **130**, 187–201.

JOP, P., FORTERRE, Y. & POULIQUEN, O. 2006 A constitutive law for dense granular flows. *Nature* **441**, 727–730.

LIM, K. S. & AGARWAL, P. K. 1994 Circulatory motion of a large and lighter sphere in a bubbling fluidized bed of smaller and heavier particles **49**, 421–424.

LUN, C. K. K., SAVAGE, S. B., JEFFREY, D. J. & CHEPURNIY, N. 1984 Kinetic theories for granular flow: inelastic particles in couette flow and slightly inelastic particles in a flow field. *Journal of Fluid Mechanics* **140**, 233–256.

MÜ1LLER, C. R., DAVIDSON, J. F., DENNIS, J. S. & HAYHURST, A. N. 2007 A study of the motion and eruption of a bubble at the surface of a two-dimensional fluidized bed using particle image velocimetry (piv). *Ind. Eng. Chem. Res.* **46**, 1642–1652.

NIENOW, A. W., ROWE, P. N. & CHIBA, T. 1978 Mixing and segregation of a small portion of large particles in gas fluidized beds of considerably smaller ones. *AIChE Symposium Series* **74**, 45–53.

NIKLASSON, F., THUNMAN, H. & LECKNER, B. 2002 Estimation of solids mixing in a fluidized-bed combustor. *Industrial and Engineering Chemistry Research* **41**, 4663–4673.

PALLARÈS, D., DIAZ, P. A. & JOHNSSON, F. 2007 Experimental analysis of fuel mixing pattern in a fluidized bed. *12th International Conference on Fluidization* **Harrison, Canada**, 929–936.

PALLARÈS, D. & JOHNSSON, F. 2006 A novel technique for particle tracking in cold 2-dimensional fluidized beds-simulating fuel dispersion **61**, 2710–2720.

PASSALACQUA, A. & MARMO, L. 2009 A critical comparison of frictional stress models applied to the simulation of bubbling fluidized beds. *Chemical Engineering Science* **64**, 2795–2806.

PEIRANO, E., DELLOUME, V., JOHNSSON, F., LECKNER, B. & SIMONIN, O. 2002 Numerical simulation of the fluid dynamics of a freely bubbling fluidized bed: influence of the air supply system. *Powder Technology* **122**, 69–82.

RIOS, G. M., TRAN, K. D. & MASSON, H. 1986 Free object motion in a gas fluidized bed. *Chemical Engineering Communications* **47**, 247–272.

SASIC, S., JOHNSSON, F. & LECKNER, B. 2006 Inlet boundary conditions for the simulation of fluid dynamics in gas-solid fluidized beds **61**, 5183–5195.

SCHAEFFER, D. G. 1987 Instability in the evolution equations describing incompressible granular flow. *Journal of Differential Equations* **66**, 61–74.

SCHILLER, L. & NAUMAN, A. Z. 1933 Uber die grundlegenden berechnungen bei der schwerkraftaufbereitung. *Vereins deutcher Ing* **77**, 310–320.

SRIVASTAVA, A. & SUNDARESAN, S. 2003 Analysis of a frictional–kinetic model for ga–particle flow. *Powder Technology* **129**, 72–85.

SUNG, W. & STELL, G. 1982 Transport theory of binary mixture with one trace component of disparate mass. *The Journal of Chemical Physics* **77**, 4636–4649.

SVENSSON, A., JOHNSSON, F. & LECKNER, B. 1996 Fluidization regimes in non-slugging fluidized beds: the influence of pressure drop across the air distributor. *Powder Technology* **86**, 299–312.

SYAMLAL, M., ROGERS, W. & O'BRIEN, T. 1993 MFIX documentation and theory guide, DOE/METC94/1004, NTIS DE94000087. U.S. Department of Energy, Office of Fossil Energy, Morgantown, WV. (also, see https://mfix.netl.doe.gov) .

TSUJI, Y. & T. KAWAGUCHI, T. T. 1993 Discrete particle simulation of two-dimensional fluidized bed. *Powder Technology* **77**, 79–87.

VAN WACHEM, B. G. M., SCHOUTEN, J. C., VAN DEN BLEEK, C. M., KRISHNA, R. & SINCLAIR, J. L. 2001 Comparative analysis of CFD models of dense gas–solid systems. *AIChE Journal* **47**, 1035–1051.

WEN, C. Y. & YU, Y. H. 1966 A generalized method for predicting the minimum fluidization velocity. *AIChE Journal* **12**, 610–612.

XIANG, Q., NI, G., CEN, K. & TAO, T. 1987 Lateral dispersion of large coal particles in an industrial-scale fluidized bed combustor. pp. 546–553. Proceedings of the Ninth International Conference on Fluidized Bed Combustion, Boston.